Kovove Mater. 51 2013 189–196
DOI: 10.4149/km_2013_3_189

Effect of heat treatment on structure and properties of B alloyed high speed steel for rolling mill rolls

H. G. Fu[1]*, Z. Z. Du[2], Y. Jiang[3], P. Li[2], R. Zhou[3], Q. H. Cen[3], Y. P. Lei[1], J. D. Xing[4]

[1]*School of Materials Science and Engineering, Beijing University of Technology, Number 100, Pingle Garden, Chaoyang District, Beijing 100124, P. R. China*
[2]*School of Metallurgical Engineering, Xi'an University of Architecture and Technology, Xi'an 710055, Shaanxi Province, P. R. China*
[3]*School of Materials Science and Engineering, Kunming University of Science and Technology, Kunming 650093, Yunnan Province, P. R. China*
[4]*School of Materials Science and Engineering, Xi'an Jiaotong University, Xi'an 710049, Shaanxi Province, P. R. China*

Received 18 April 2012, received in revised form 9. October 2012, accepted 11 June 2013

Abstract

Solidification structure of two kinds of B alloyed high speed steel for rolling mill rolls, which carbon contents are 0.50 % and 1.00 %, respectively, and the changes in the microstructure and mechanical properties after quenching from 1050 °C and tempering at 200–600 °C, respectively, are studied. The results of metallographic, scanning electron microscopy analysis, X-ray diffraction analysis, hardness and impact toughness measurements of as-cast and heat-treated B alloyed high speed steel are discussed. As-cast matrix of B alloyed high speed steel consists of martensite and troostite. There are 19–26 vol.% $M_{23}(B, C)_6$, $M_3(B_{0.7}C_{0.3})$ and $M_2(B, C)$ type carboborides in the matrix. Microhardness values of $M_{23}(B, C)_6$, $M_3(B_{0.7}C_{0.3})$ and $M_2(B, C)$ are 1940–2030 HV, 1380–1460 HV and 1460–1530 HV, respectively. Macrohardness of as-cast B alloyed high speed steel reaches 58–60 HRC. After quenching from 1050 °C, the eutectic $M_{23}(B, C)_6$ and $M_3(B_{0.7}C_{0.3})$ carboborides dissolve into the matrix, and many granular $M_{23}(B, C)_6$ precipitate from the matrix, and the whole matrix transforms into martensite. Microhardness of matrix and macrohardness of quenched B alloyed high speed steel have a slight increase comparing with as-cast sample. Hardness of the B alloyed high speed steel remains constant while tempering temperature is below 550 °C, and then, with increasing temperature, decreases considerably. Impact toughness of the B alloyed high speed steel increases slightly until tempering temperature reaches 525 °C, and then increases considerably. B alloyed high speed steel has higher hardness and has an excellent wear resistance after tempering under 550 °C that can be attributed to the effect of boron.

K e y w o r d s: high speed steel for rolling mill roll, B alloyed steel, carboboride, quenching, tempering, hardness, impact toughness

1. Introduction

The rolling mill productivity, as well as the surface quality, shape and roughness of the rolled product, are all directly affected by the time that the roll can be in operation before removal due to deterioration in both the structure and properties. In most cases, work rolls for the finishing stands of hot rolling mills are high chromium (HiCr) and indefinite chill iron (IC) rolls [1, 2]. However, over the last 20 years high speed steel rolls produced by centrifugal casting are used in hot rolling mills instead of HiCr and IC rolls due to their superior mechanical properties such as high hardness and strong wear resistance, which are kept at high temperature [3–6]. The use of the high speed steel rolls results in their extended tool life and enhanced surface quality of the rolled products [6–8].

High speed steel roll materials are complex multi--component alloys, with a carbon content ranging from 1.5 to 2.5 mass% and significant amount of alloy

*Corresponding author: tel.: +86-10-67396244; fax: +86-10-67396093; e-mail address: fhg64@263.net

Table 1. Chemical composition of B-HSS roll shell (wt.%)

Sample	C	B	W	Mo	Cr	V	Si	Mn	S	P	Fe
A1	0.48	1.17	0.93	1.10	4.95	0.55	0.75	0.36	0.029	0.033	Bal.
A2	0.95	1.16	0.96	1.06	4.94	0.51	0.75	0.38	0.030	0.032	Bal.

elements such as vanadium, tungsten, chromium and molybdenum. The typical compositions of high speed steel rolls consist of 1.5–2.5 % C, up to 6 % W, 6 % Mo, 3–8 % Cr and 4–10 % V [9, 10]. However, tungsten, molybdenum and vanadium, etc., are costly alloy elements. The addition of tungsten, molybdenum and vanadium increases rapidly the production cost of the high speed steel rolls, which restricts their application.

Boron is low-cost and useful as an alloying element in many materials. Boron is added to unalloyed and low alloyed steels in very small amounts (in ppm range), to enhance hardness level through the hardenability enhancement [11–17]. Boron added to high-speed-cut steels, for example, containing 18 % W, 4 % Cr and 1 % V, enhances their cutting performance. Chaus [18, 19] investigated thoroughly the structural changes during heat treatments in the high-speed steels alloyed with boron (M2 and M35 grades, and high chromium high-speed steels) and reported that the high-speed steels with an optimum boron content, being somewhat inferior to the base steels in the impact toughness, were considerably superior to those in the wear and heat resistance.

The aim of the present work is to substitute partial tungsten, molybdenum and vanadium by boron in high speed steel for rolls, and develop a kind of cheap B alloyed High Speed Steel (B-HSS), main composition of which is 0.50–1.00 % C, 1.0 % W, 1.0 % Mo, 0.5 % V, 5.0 % Cr and 1.2 % B. However, the heat treatment process of the B-HSS has no more reports besides the introduction of Chaus [18, 19]. This paper also presents the changes in the microstructure and mechanical properties of B-HSS after quenching from 1050 ℃ and tempering at 200–600 ℃, that can provide useful information on the developed heat-treatment cycle when the B-HSS will be used in industry.

2. Experimental

2.1. Sample preparation

The B-HSS was smelted in a medium frequency induction furnace of 350 kg capacity using carburant, low carbon steel, ferrovanadium, ferrotungsten, ferromolybdenum, ferroboron, ferrochromium, ferrosilicon and ferromanganese. After being deoxidized with 0.10–0.12 % Al, at 1600–1620 ℃ the molten steel was discharged into a pre-heated ladle. The B-HSS rolls were manufactured in a horizontal centrifugal casting apparatus. At 1460–1480 ℃, the melt was poured into a high-speed revolving mould to form a shell part. The thickness of the shell wall was 60 mm. After revolving 8–10 min, the mould containing B-HSS roll shell was detached from the centrifuge. Afterward, undercasing and top box were combined together. At last the spheroidal graphite liquid of roll centre was filled. Dimensions of B-HSS roll were ø 350 mm × 2830 mm. Final chemical composition of the B-HSS roll shell is introduced in Table 1. Figure 1 shows diagrammatic sketch of the B-HSS compound roll.

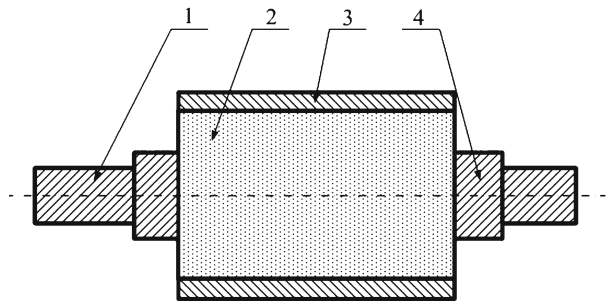

Fig. 1. Diagrammatic sketch of B-HSS compound roll: 1 – upper roll neck, 2 – spheroidal graphite of roll centre, 3 – B-HSS shell; 4 – lower roll neck.

Specimens for heat treatment test were cut down from the shell of the B-HSS compound roll. Dimensions of the specimens were 11 mm × 11 mm × 55 mm. The specimens were heated to 1050 ℃ and held for 1 h in a vacuum furnace with a vacuum limit of 6.7×10^{-2} Pa, and then quenched by oil cooling to room temperature. The main reason that the duration was 1 h was as follows. Because there was a lot of carboboride in as-cast B-HSS, longer duration could increase the contents of boron and alloy elements in the matrix and improve the hardenability of B-HSS. Tempering of the samples was done at 200 ℃, 300 ℃, 400 ℃, 500 ℃, 525 ℃, 550 ℃, and 600 ℃, respectively, with constant holding time 3 h, followed by cooling to room temperature in still air.

2.2. Microstructure examination

Investigation techniques used for B-HSS microstructure characterization included X-ray diffraction (XRD), optical microscopy (OM), and scanning electron microscopy (SEM). Samples were etched with 5 %

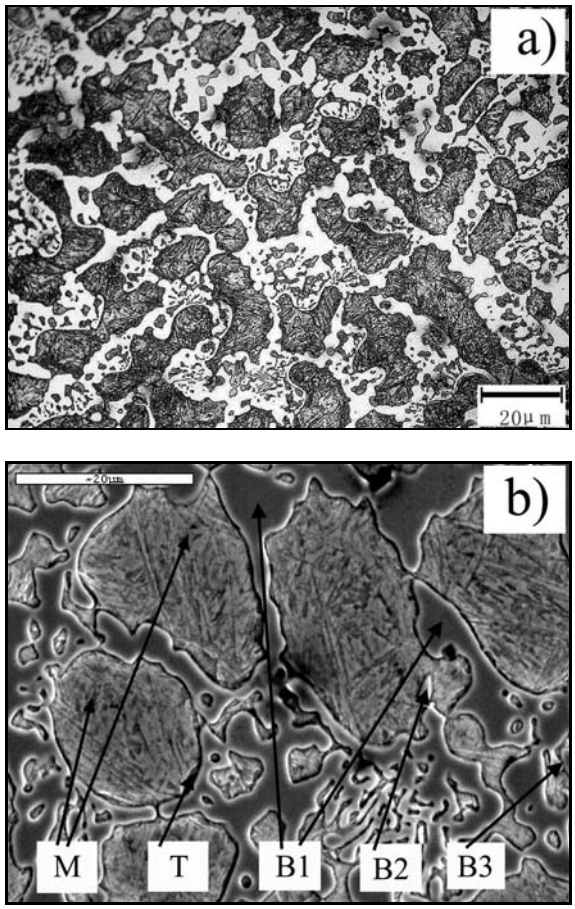

Fig. 2. OM (a) and SEM (b) images of as-cast A1 sample: B1 – M_2(B, C), B2 – M_{23}(B, C)$_6$, B3 – $M_3(B_{0.7}C_{0.3})$, M – martensite, T – troostite.

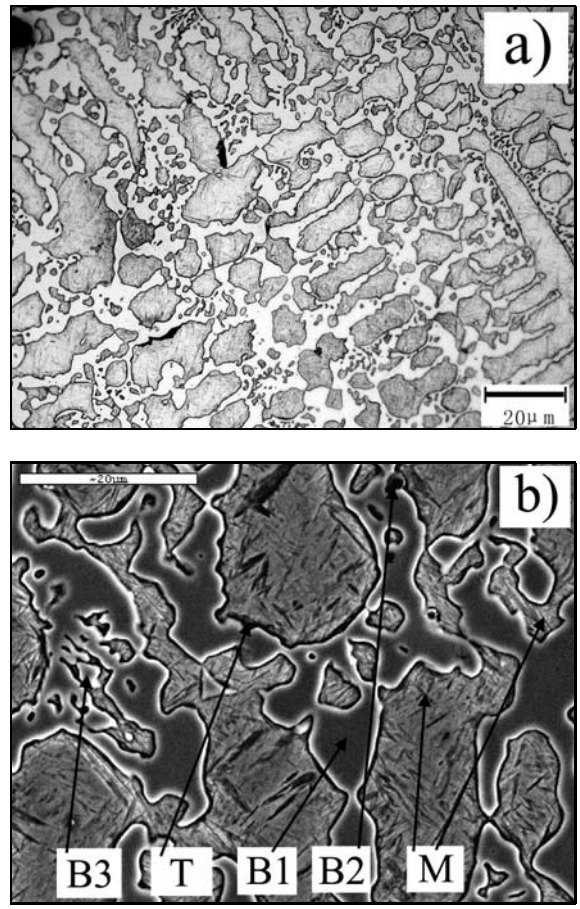

Fig. 3. OM (a) and SEM (b) images of as-cast A2 sample: B1 – M_2(B, C), B2 – M_{23}(B, C)$_6$, B3 – $M_3(B_{0.7}C_{0.3})$, M – martensite, T – troostite.

nital for optical microscopy examination, while a mixture of 5cc HCl, 45cc 4 % picral and 50cc 5 % nital was used as an etchant for SEM evaluation. XRD was performed on the bulk material of B-HSS specimens and was carried on a M21X diffractometer with copper Kα radiation at 40 kV and 200 mA as an X-ray source. Sample was scanned in the 2θ range of 10°–90° in a step-scan mode (0.02° per step). According to the method put forward by Zhi and Xing [20, 21], the measurement of volume fraction of carboborides used a Leica digital images analyzer on the deep etched specimens.

2.3. Mechanical performance tests

Impact toughness was performed on a JBN-300B type impact tester, the dimensions of unnotched specimens were 10 mm × 10 mm × 55 mm. Impact load was 294 N. Impact toughness values were the average of three specimens. Macrohardness testing was done using an HR-150C type hardmeter. Microhardness was measured using a HX-1000TM type Vickers microhardness tester and a load of 0.5 N. At least seven indentations were made on each sample under each experimental condition to check the reproducibility of hardness data.

3. Results and discussion

3.1. Solidification microstructure of B-HSS

The solidification structures of B-HSS are shown in Figs. 2 and 3. As-cast solidification structures of B-HSS consist of metallic matrix and carboborides, and the volume fractions of carboborides in A1 sample and A2 sample are about 19–21 vol.% and 24–26 vol.%, respectively. XRD spectrum of Fig. 4 shows that the carboborides in solidification structures of B-HSS are M_{23}(B, C)$_6$, $M_3(B_{0.7}C_{0.3})$ and M_2(B, C), therefore M represents Fe, Cr, W, Mo, Mn and V, etc., elements. The amount of M_{23}(B, C)$_6$ is the least and that of M_2(B, C) is the most. Microhardness values of M_{23}(B, C)$_6$, $M_3(B_{0.7}C_{0.3})$ and M_2(B, C) are

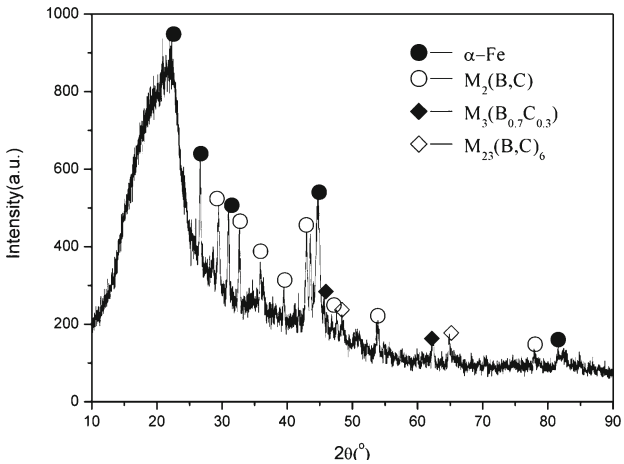

Fig. 4. XRD spectrum of as-cast A1 sample.

1940–2030 HV, 1380–1460 HV and 1460–1530 HV, respectively. XRD spectrum of Fig. 4 approves also that the metallic matrix is α-Fe. However, the microhardness value of metallic matrix at different place has considerable difference. The microhardness of metallic matrix apart from eutectic carboborides is higher and reaches 680–730 HV, and the microhardness of metallic matrix close to eutectic carboborides is lower, and is 450–510 HV only. So, the former is martensite and the latter is troostite, and as-cast matrix of B-HSS consists of martensite and troostite. Macrohardness values of as-cast A1 and A2 samples are 58.3 HRC and 60.6 HRC, and their impact toughness values are 56 kJ m^{-2} and 50 kJ m^{-2}, respectively. Moreover, M_2(B, C) and $M_3(B_{0.7}C_{0.3})$ type carboborides are continuously distributed over the grain boundary.

3.2. Microstructure and properties of quenched B-HSS

According to the manufacture characteristics of centrifugal casting high speed steel compound roll and the experience [4, 22], the austenitizing temperature of

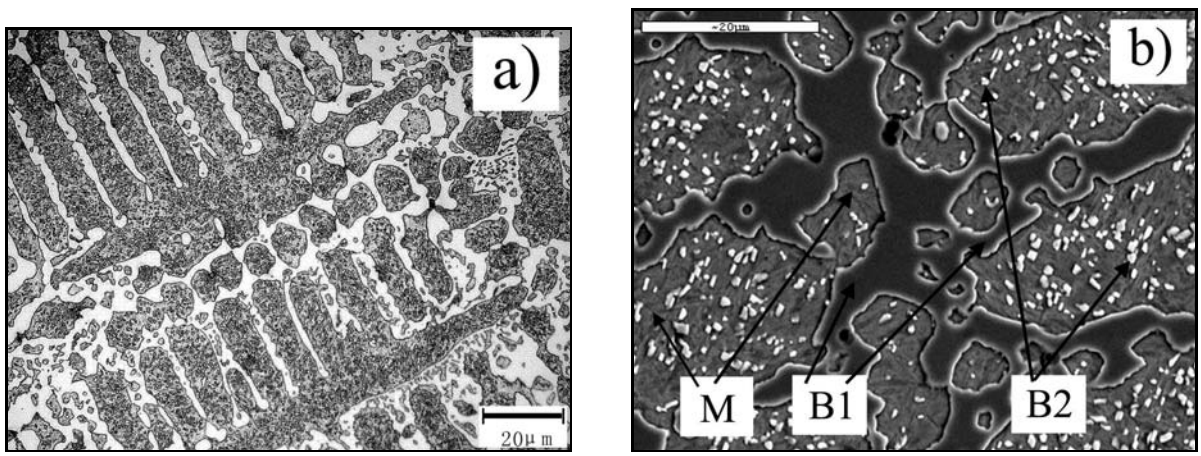

Fig. 5. OM (a) and SEM (b) images of A1 quenched sample: B1 – M_2(B, C), B2 – granular M_{23}(B, C)$_6$, M – quenched martensite.

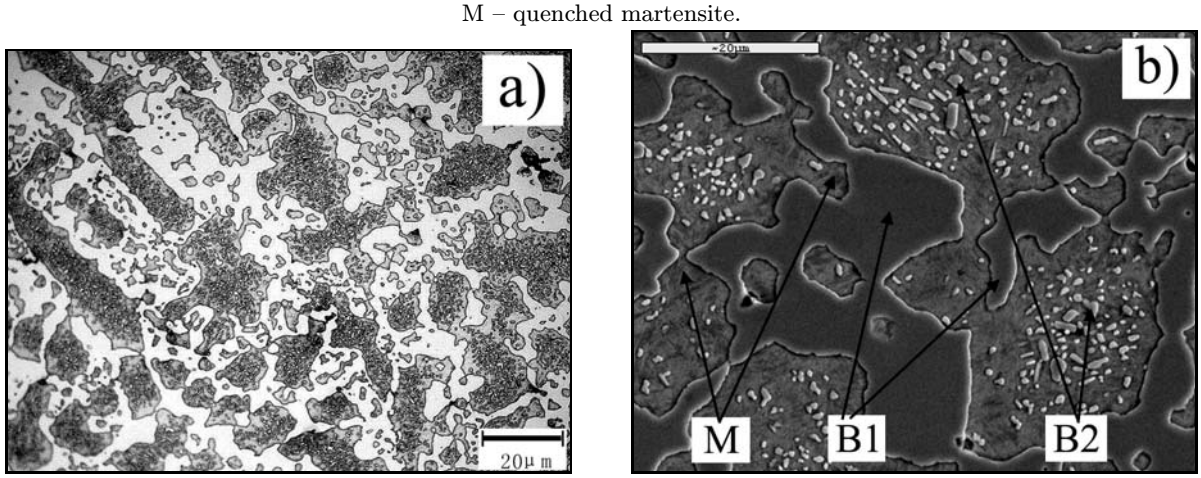

Fig. 6. OM (a) and SEM (b) images of A2 quenched sample: B1 – M_2(B, C), B2 – granular M_{23}(B, C)$_6$, M – quenched martensite.

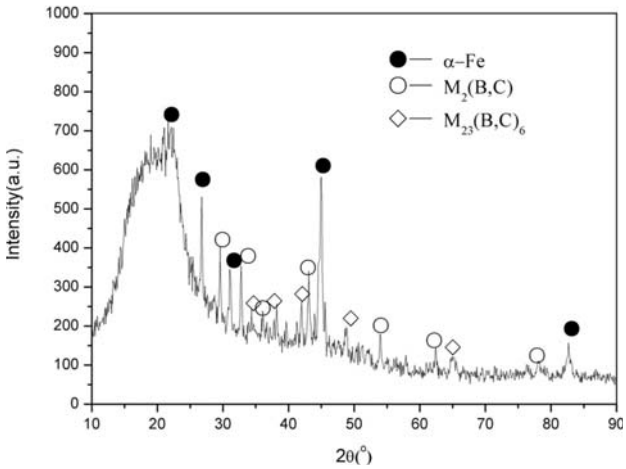

Fig. 7. XRD spectrum of A1 sample quenched from 1050 °C.

B-HSS roll sample was selected 1050 °C. The quenched microstructures of B-HSS are shown in Figs. 5 and 6. Moreover, eutectic $M_{23}(B, C)_6$ and $M_3(B_{0.7}C_{0.3})$ carboborides dissolve into the matrix, and many granular carboborides precipitate from the matrix, and the whole matrix transforms into martensite after quenching from 1050 °C. The XRD spectrum in Fig. 7 shows that precipitated particles are $M_{23}(B, C)_6$ type carboborides.

During the quenching heat treatment, qualitative and quantitative changes in the carboboride constituent of B-HSS, caused by diffusion and mass transfer, take place. They are related to the diffusion redistribution of the alloying elements between steel matrix and carboboride phases that leads to the dissolution of existing phases and formation of new ones. In particular, after solution-treated at 1050 °C, the amount of $M_{23}(B, C)_6$ carboboride increases considerably. This is most likely to be caused by the $M_2(B, C) \rightarrow M_{23}(B, C)_6$ transformation.

Microhardness of matrix and macrohardness of B-HSS have a slight increase comparing with as-cast sample and reach 720–750 HV and 62–64 HRC, respectively. However, the impact toughness of B-HSS after quenching has a slight decrease. The impact toughness of A1 and A2 sample are 46 kJ m^{-2} and 43 kJ m^{-2}, respectively, because of the existence of quenching internal stress.

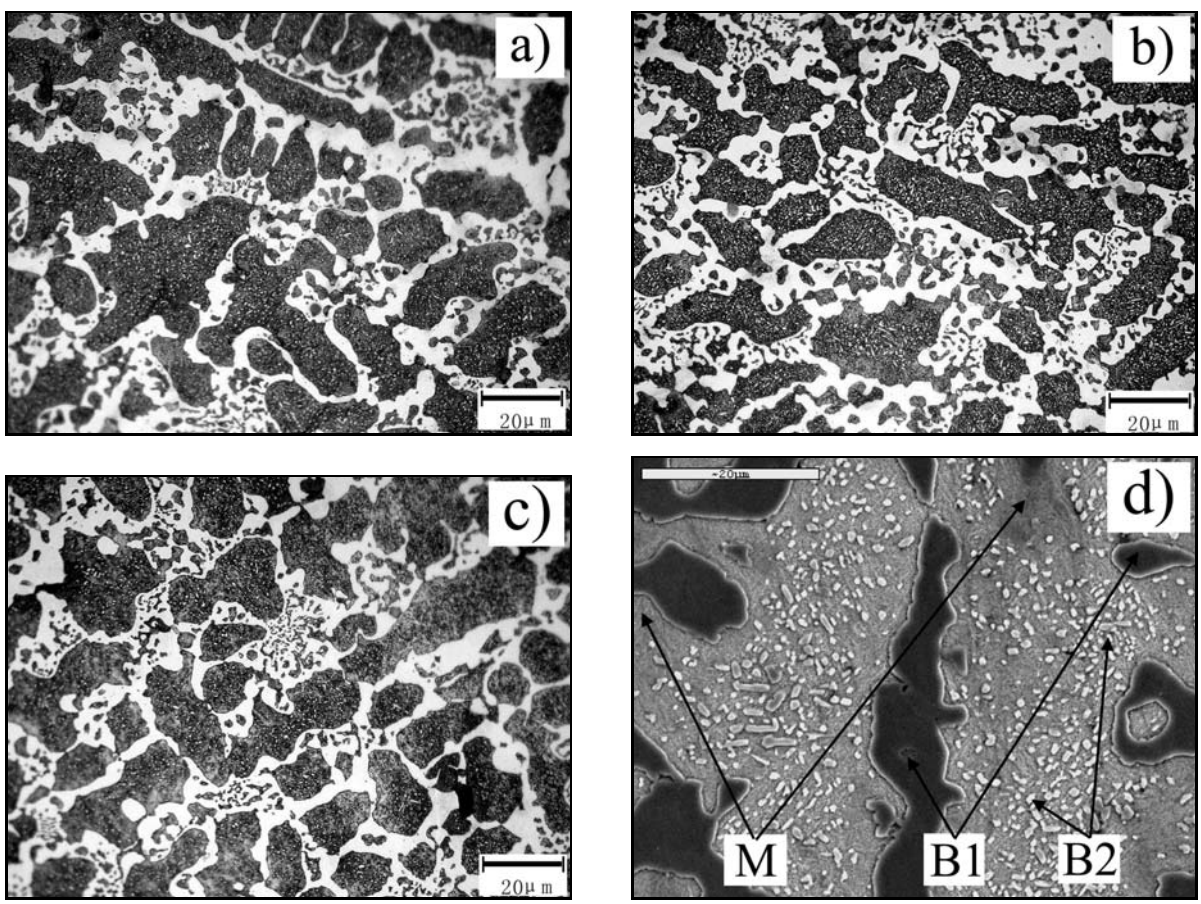

Fig. 8. OM images of A1 sample tempered at 200 °C (a), 550 °C (b) and 600 °C (c), SEM image of A1 sample tempered at 550 °C (d): M – tempered martensite; B1 – $M_2(B, C)$, B2 – granular $M_{23}(B, C)_6$.

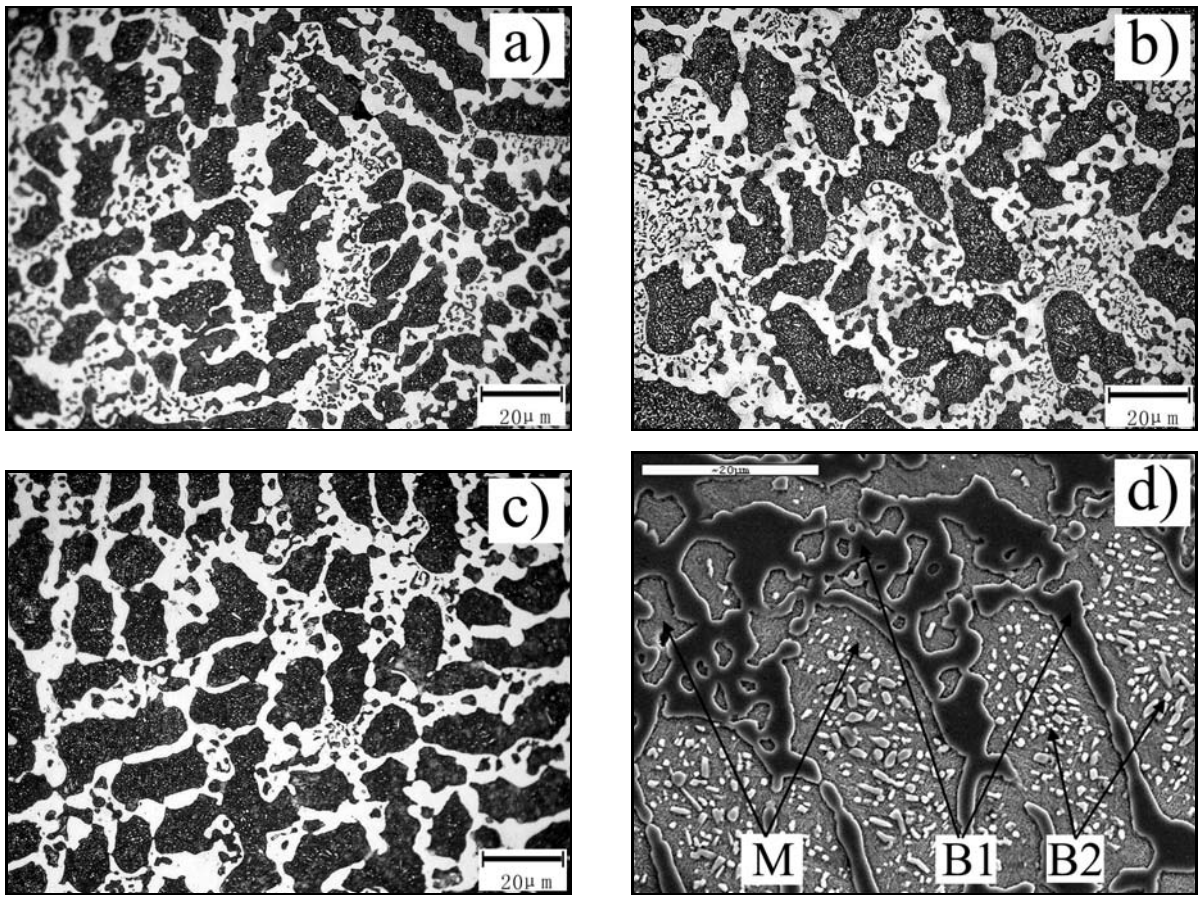

Fig. 9. OM images of A2 sample tempered at 200 ℃ (a), 550 ℃ (b) and 600 ℃ (c), SEM image of A2 sample tempered at 550 ℃ (d): M – tempered martensite, B1 – M_2(B, C), B2 – granular M_{23}(B, C)$_6$.

3.3. Effect of tempering temperature on microstructure and properties of B-HSS

Microstructures of B-HSS quenched from 1050 ℃ and tempered at 200 ℃, 550 ℃ and 600 ℃, respectively, are shown in Figs. 8 and 9. When tempering temperature is lower, microstructure of B-HSS has no obvious change. Comparison of Figs. 5b and 6b with Figs. 8d and 9d shows that the amount of precipitated carboboride particles increases with increasing tempering temperature. Moreover, all quenched martensite transforms into the tempered martensite after tempering. XRD spectrum of Fig. 10 shows that carboboride types are not changed after tempering, and the carboborides consist of eutectic M_2(B, C) and granular M_{23}(B, C)$_6$.

Figure 11 shows that the hardness of investigated alloys after tempering to 550 ℃ is nearly constant of 60 HRC. When tempering temperature exceeds 550 ℃, the hardness begins to decrease. This shows B-HSS has an excellent wear resistance after tempering under 550 ℃. Effect of tempering temperature on wear resistance of B-HSS roll alloy will be studied in future experiments. Common high-speed tool steel has strong secondary hardening after tempering because of the precipitation of secondary alloy carbides and more complete transformation of retained austenite [23–26]. However, the quenching temperature of investigated B-HSS is only 1050 ℃, and there is little retained austenite in quenched structure. When

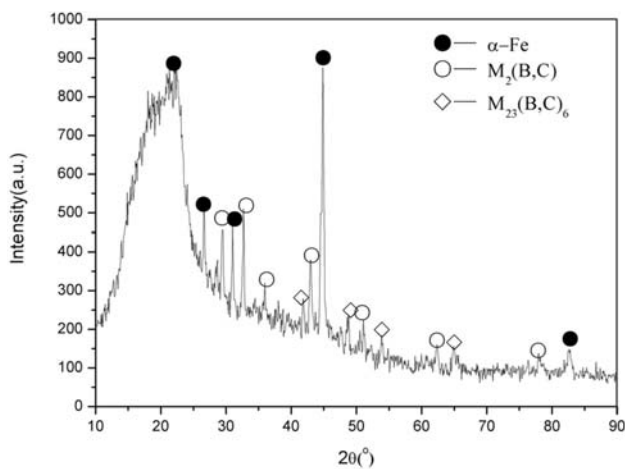

Fig. 10. XRD spectrum of A1 sample quenched from 1050 ℃ and tempered at 550 ℃.

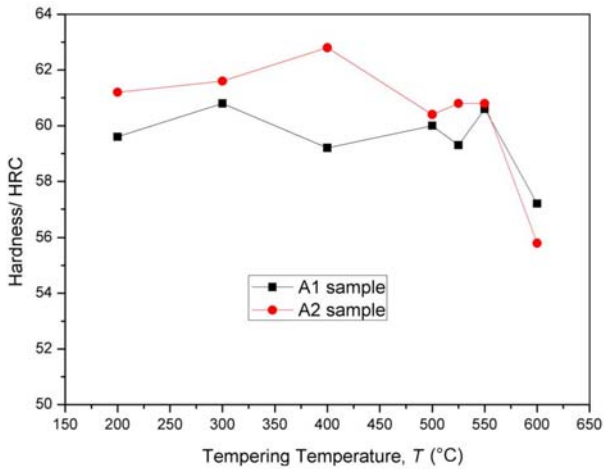

Fig. 11. Effect of tempering temperature on the hardness of B-HSS.

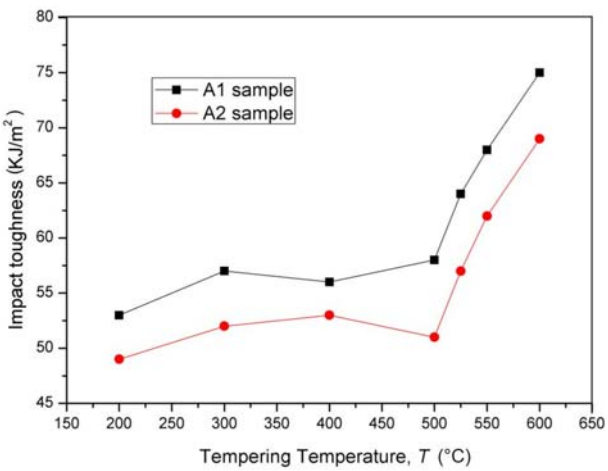

Fig. 12. Effect of tempering temperature on the impact toughness of B-HSS.

B-HSS is tempered below 550 ℃, there is no obvious secondary hardening. When tempering temperature increases further, alloy carboborides precipitated from the matrix begin to grow and coarsen, which leads to the decrease of hardness.

Figure 12 shows the effect of tempering temperature on impact toughness of B-HSS. By comparing with the quenched sample, the impact toughness of B-HSS increases considerably after tempering. The impact toughness of B-HSS increases slightly until tempering temperature reaches 525 ℃, and then increases considerably. Because the amount of eutectic carboboride in A2 sample is more than that in A1 sample and the eutectic carboboride is a brittle phase, so impact toughness of A2 sample is lower than that of A1 sample. B alloyed high speed steel has higher hardness and has an excellent wear resistance after tempering under 550 ℃ that can be attributed to the effect of boron.

4. Conclusions

Based on the above results, following conclusions can be drawn:

1. Solidification microstructure of B-HSS containing 0.5–1.0 % C, 1.0 % W, 1.0 % Mo, 0.5 % V, 5.0 % Cr and 1.2 % B consists of martensite, troostite, and $M_{23}(B, C)_6$, $M_3(B_{0.7}C_{0.3})$ and $M_2(B, C)$ type carboborides.

2. Eutectic $M_{23}(B, C)_6$ and $M_3(B_{0.7}C_{0.3})$ carboborides dissolve into the matrix, and many granular carboborides precipitate from the matrix, and the whole matrix transforms into martensite after quenching from 1050 ℃.

3. When tempering temperature is lower, microstructure of B-HSS has no obvious change, and the amount of granular carboborides precipitating from matrix increases while tempering temperature increases.

4. Hardness of B-HSS has no obvious change after tempering under 550 ℃. Its impact toughness increases slightly until tempering temperature reaches 525 ℃, and then increases considerably.

Acknowledgements

The authors would like to thank the financial support for this work from Scientific Plan Item of Beijing Education Committee (PXM2012-014204-00-000136, PXM2012--014204-00-000156), National Natural Science Foundation of China under grant (51054008), and Yunnan Province Science and Technology Cooperating Item under grant (2010AD012).

References

[1] Skoblo, T. S., Vishnyakova, E. N., Mozharova, N. M., Dubrov, V. A., Bondin, R. D.: Metal Science and Heat Treatment, *32*, 1991, p. 734. doi:10.1007/BF00693690

[2] Andersson, M., Finnstrom, R., Nylen, T.: Ironmaking & Steelmaking, 2004, *31*, p. 383. doi:10.1179/030192304225018208

[3] Ichino, K., Ishikawa, S., Kataoka, Y., Toyooka, T.: Journal of the Iron and Steel Institute of Japan, *89*, 2003, p. 680.

[4] Fu, H. G., Xing, J. D.: Manufacture Technology of High Speed Steel Roll. Beijing, Metallurgical Industry Press 2007.

[5] Xavier, R. R., de Carvalho, M. A., Cannizza, E., White, T. H., Rivaroli, A., Jr., Sinatora, A.: Iron & Steel Technology, *1*, 2004, p. 28.

[6] Takigawa, H., Ohtomo, S., Tanaka, T., Hashimoto, M.: Nippon Steel Technical Report, *74*, 1997, p. 77.

[7] Tsuchihashi, T., Sato, J., Shiraishi, T., Kawashima, T., Hirata, K.: Research and Development Kobe Steel Engineering Reports, *48*, 1998, p. 10.
[8] Sano, Y., Hattori, T., Haga, M.: ISIJ International, *32*, 1992, p. 1194. doi:10.2355/isijinternational.32.1194
[9] Park, J. W., Lee, H. C., Lee, S.: Metallurgical and Materials Transactions A, *30A*, 1999, p. 399.
[10] Pellizzari, M., Cescato, D., Straffelini, G., Valentini, R., Solina, A.: Metallurgia Italiana, *100*, 2008, p. 17.
[11] Chen, Z., Wu, X. C., Wang, H. B., Min, Y. A., Zhang, H. K.: Journal of Iron and Steel Research, *20*, 2008, p. 40.
[12] Fu, H. G., Zou, D. N., Jiang, Z. Q., Yang, J., Wang, J. H., Xing, J. D.: Materials and Manufacturing Processes, *23*, 2008, p. 469. doi:10.1080/10426910802103775
[13] Jimenez, J. A., Acosta, P., Frommeyer, G., Ruano, O. A.: Zeitschrift für Metallkunde, *86*, 1995, p. 693.
[14] Jimenez, J. A., Frommeyer, G., Acosta, P., Ruano, O. A.: Materials Science and Engineering, *A202*, 1995, p. 94. doi:10.1016/0921-5093(95)09799-6
[15] Acosta, P., Jimenez, J. A., Ruano, O. A.: Steel Research, *66*, 1995, p. 360.
[16] Fu, H. G., Yan, L. F., Jiang, Z. Q., Xing, J. D.: International Journal of Materials Research, *98*, 2007, p. 521.
[17] Spiridonova, I. M.: Metallovedenie i termicheskaya obrabotka metallov, 1984, p. 58.
[18] Chaus, A. S.: Physics of Metals and Metallography, *91*, 2001, p. 463.
[19] Chaus, A. S.: Physics of Metals and Metallography, *106*, 2008, p. 82. doi:10.1134/S0031918X08070119
[20] Zhi, X. H., Xing, J. D., Gao, Y. M., Fu, H. G., Peng, J. Y., Xiao, B.: Materials Science and Engineering A, *487*, 2008, p. 171. doi:10.1016/j.msea.2007.10.009
[21] Fu, H. G., Li, Z. H., Jiang, Z. Q., Xing, J. D.: Materials Letters, *61*, 2007, p. 4504. doi:10.1016/j.matlet.2007.02.037
[22] Fu, H. G., Qu, Y. H, Xing, J. D., Zhi, X. H., Jiang, Z. Q., Li, M. W., Zhang, Y.: Journal of Materials Engineering and Performance, *17*, 2008, p. 535. doi:10.1007/s11665-007-9174-4
[23] Chaus, A. S., Rudnickii, F. I.: Defect and Diffusion Forum, *297–301*, 2010, p. 1071. doi:10.4028/www.scientific.net/DDF.297-301.1071
[24] Moon, H. K., Lee, K. B., Kwon, H.: Materials Science & Engineering A, *474*, 2008, p. 328. doi:10.1016/j.msea.2007.04.014
[25] Qiu, J., Yuan, Y., Chen, J. R.: Acta Metallurgica Sinica, *28*, 1992, p. 301.
[26] Karagoez, S., Andren, H. O.: Zeitschrift für Metallkunde, *83*, 1992, p. 386.